Supplementary materials

0.1. The Matsui potential for silicate systems

The Matsui (1998) potential model in its original form can be represented by the following equation:

$$V(r_{ij}) = \frac{q_i q_j}{r_{ij}} - \frac{C_j C_j}{r_{ij}^6} + f\,(B_i + B_j) \exp\left(\frac{A_i + A_j - r_{ij}}{B_i + B_j}\right) \tag{1}$$

From left to right, the three terms describes Coulomb interaction, van der Waals attraction and Born-Mayer-Huggins repulsion, respectively. Born-Mayer-Huggins repulsion is a soft-sphere model for closed-shell atoms and ions published by Gilbert (1968). The physical meaning of f in this term is an arbitrary standard force by which the atom pairs are pushed apart until the distance between them is the sum of their soft-core radius. Matsui set his standard force to be 4.184 kJ $\text{Å}^{-1}\text{mol}^{-1}$. The soft-core radius of atom i and j are denoted by A_i and A_j, respectively. B_i and B_j are called softness (or hardness) parameters.
To simplify the form of this pairwise potential, we can perform the following transformations to equation 1.

$$C_{ij} = C_i * C_j \tag{2}$$

$$B_{ij} = B_i + B_j \tag{3}$$

$$A_{ij} = f B_{ij} \exp\left(\frac{A_i + A_j}{B_{ij}}\right) \tag{4}$$

And we can get a new form as follows.

$$V(r_{ij}) = \frac{q_i q_j e^2}{4\pi\epsilon_0 r_{ij}} + A_{ij} \exp\left(-\frac{r_{ij}}{B_{ij}}\right) - \frac{C_{ij}}{r_{ij}^6} \tag{5}$$

In this new form, A_{ij} and C_{ij} are called energy parameters for the pair ij and they describe the repulsive and van der Waals attractive forces, respectively. B_{ij} is an e-folding length characterizing the radially symmetric decay of electron repulsion energy between atom pair ij. The second and third terms together are known as a Buckingham potential.
In LAMMPS, this pairwise potential can be described by the built-in buck/coul/long pair style.

$$E_{\text{Buck}} = Ae^{-r/\eta} - \frac{C}{r^6},\ r < r_c \tag{6}$$

$$E_{\text{Coul}} = \frac{Cq_i q_j}{\epsilon r},\ r < r_c \tag{7}$$

$$E_{total} = E_{\text{Buck}} + E_{\text{Coul}} \tag{8}$$

In our force field optimizations, we started from the parameters given by Matsui (1998) and modified the van der Waals part (E_{Buck}) only.
In all simulations, we used PPPM long-range interactions for the Coulomb potential and set the cut-off radius for the Buckingham potential to be r_c =11 Å.

0.2. Transformation of Buckingham potential

To understand the physical meanings of the optimization parameters and make more precise adjustments, we transformed the van der Waals part of the pairwise potential according to the exponential-6 (X6) form (Mayo, Olafson and Goddard, 1990).

$$E_{\mathrm{vdw}}^{\mathrm{X6}} = D_0 \left[\frac{6}{\zeta - 6} e^{\zeta(1-\rho)} - \frac{\zeta}{\zeta - 6} \rho^{-6} \right] \tag{9}$$

where D_0 is the van der Waals well depth, $\rho = R/R_0$ is relative bond length where R_0 is equilibrium bond length and ζ is a dimensionless scaling parameter. $\zeta = 12.0$ means the X6 form and the LJ form have the same long range interactions and $\zeta = 13.772$ means they have the same force constant. The X6 form has advantages in describing short range interactions and is suitable for our force field where covalent and ionic bonds are dominant.
By comparing Eqn. 6 and Eqn. 9, we can find a set of solutions that represents D_0, R_0 and ζ using A, η and C. The transformation of force field parameters is automated by Python and done in Mathematica (Wolfram Research, Inc., 2020).

0.3. Optimization details

The parameters that are tuned in our optimization are the transformed Buckingham parameters D_0, R_0 and ζ for all Cat-O pairs (tuned simutaneously) and for O-O pairs. There are six parameters in total.
To avoid cancelling of different parts, we used the sum of log (e-based) losses as our optimization goal.

$$L = \log(\alpha_P L_P + \alpha_{C_V} L_{C_V} + \alpha_\gamma L_\gamma) \tag{10}$$

where L is the total loss, α's are the scaling parameters for each kind of loss and L_P, L_{C_V} and L_γ are the losses corresponding to pressure, heat capacity and Grüneisen parameter, respectively. For a simulation containing 4 reference points (which yields 4 pressures, 2 heat capacities and 2 Grüneisen parameters because the latter two are calculated by finite difference), each part of the loss function is defined as:

$$L_P = \frac{1}{4} \sum_{i=1}^{4} (P_i - P_{i,ref})^2 \tag{11}$$

$$L_{C_V} = \frac{1}{2} \sum_{i=1}^{2} (C_{Vi} - C_{Vi,ref})^2 \tag{12}$$

$$L_\gamma = \frac{1}{2} \sum_{i=1}^{2} (\gamma_i - \gamma_{i,ref})^2 \tag{13}$$

The choice of scaling parameters considers both the relative magnitude of each physical quantity and their degree of fluctuation. For our final optimizations, the choices are:

$$\alpha_P = 0.01 \tag{14}$$

$$\alpha_{C_V} = 100 \tag{15}$$

$$\alpha_\gamma = 70000000 \tag{16}$$

Both BFGS and gradient descent (GD) algorithms were used in the optimization and although BFGS reduced the loss function faster at the beginning of the optimization, the best result was produced by GD, which reduced the loss function from 3.90 to 3.59 and achieved satisfying accuracy for C_V and γ.

0.4. The force field parameters

Compared to the original Matsui force field, the optimized force field scales each parameter differently (Table S1).

The van der Waals well depth parameter (D_0) has the largest change of all, which can

Table S1: Final scaling factors of the optimized force field

Optimization paramter	Scaling=new/original
D_0(Cat-O)	0.478192
R_0(Cat-O)	0.771891
ζ(Cat-O)	1.044594
D_0(O-O)	0.684991
R_0(O-O)	0.990607
ζ(O-O)	0.804164

be attributed to the fact that high temperature and pressure conditions reduce the bond strength. For all of the oxygen-containing ion pairs, the change of equilibrium bond length (R_0) is very small, indicating that the structure of silicates can be relatively accurately described by the original force field. For Cation-Oxygen and Oxygen-Oxygen pairs, the curvature parameter (ζ) changes in opposite directions, which could be related to the difference in long range attraction between cation-anion pairs and anion-anion pairs.

These parameters are then transformed to input parameters for LAMMPS and can be found in section 0.9.

0.5. Calculating Hugoniot from Equation of State

The original Hugoniot data shown in Figure 5 were presented by Asimow and Ahrens (2010). The measured quantities in each experiment are shock velocity U_S, particle velocity u_p, and initial sample density ρ_o. These results are converted to the Pressure (P)-Density (ρ) plane using the first two Rankine-Hugoniot equations (i.e., conservation of mass and

momentum) for a single shock driven into a sample initially at zero pressure and at rest in the laboratory reference frame:

$$\rho_o U_S = \rho(U_S - u_p) \tag{17}$$

$$P = \rho_o U_S u_p. \tag{18}$$

In most of the experiments plotted, the initial state of the sample is liquid at 0.1 MPa (i.e., approximately zero) pressure at 1673 K, which is also the reference state for the equation of state adopted. One experiment begins from the initially solid state at 300 K. Interpreting this experiment requires knowing the initial density of the isochemical mixture of solids at 300 K (ρ_{OS}), as well the internal energy difference between the 1673 K liquid and 300 K solid states, ΔE_{tr}, which is the obtained from the integral of the solid heat capacity from 300 K to the eutectic temperature (1547 K), the enthalpy of fusion, and the integral of the liquid heat capacity from 1547 K to 1673 K.

These data are compared to Hugoniots computed from the thermal equation of state as follows. The independent variable is ρ. At each value of ρ, we obtain the Eulerian finite strain parameter f relative to the reference volume ρ_o:

$$f = \left\{ \left(\frac{\rho}{\rho_o} \right)^{\frac{2}{3}} - 1 \right\}. \tag{19}$$

and then the pressure on the reference isentrope is calculated from the 3$^{\text{rd}}$ order Birch-Murnaghan equation of state:

$$P_S = 3K_{oS} f (2f+1)^{\frac{5}{2}} \left[1 + \frac{3}{2}(K'_S - 4) f \right], \tag{20}$$

In which K_{oS} is the isentropic bulk modulus at the reference state (which is known precisely from ultrasonic measurements and therefore is held constant during fitting) and K'_S is the first derivative of the isentropic bulk modulus along the isentrope, evaluated at the reference state (which is not known from ambient pressure data and is therefore a fitted parameter). To obtain the pressure on the Hugoniot at shock density ρ , we take advantage of the fact that internal energy E is a path-independent state variable and therefore the difference in E between the initial reference state and the shock state is the same whether the change of state is accomplished by passage of the shock (ΔE_H) or by decomposition of the path into a series of three processes: transformation from the initial state to the reference state at 1 bar (ΔE_{tr}, if necessary), isentropic compression from the reference state at ρ_o to the shock density ρ (ΔE_S) and finally isochoric heating from the isentrope to the corresponding state on the Hugoniot (ΔE_V). That is:

$$\Delta E_H = \Delta E_{tr} + \Delta E_S + \Delta E_V. \tag{21}$$

The increase in internal energy imparted by passage of a shock is obtained from the 3$^{\text{rd}}$ Rankine-Hugoniot jump condition:

$$\Delta E_H = \frac{1}{2}(P + P_o) \left(\frac{1}{\rho_{oo}} - \frac{1}{\rho} \right), \tag{22}$$

in which ambient pressure P_o is negligible compared to shock pressure P and ρ_{oo} is the density of the initial state, which may be equal to ρ_o if the sample begins in the reference state, ρ_{os} for the case where the initial state is a cold solid assemblage, or any other value as appropriate (e.g. for a porous target).

From the first and second laws of thermodynamics, the total derivative of specific internal energy $\mathrm{d}E = T\mathrm{d}S - P\mathrm{d}V$, where T is temperature, S is specific entropy, and V is specific volume ($V = 1/\rho$). Hence, the increase in internal energy along an isentropic path (for which $\mathrm{d}S = 0$) is obtained by integrating equation (20):

$$\Delta E_S = \frac{9}{2}\frac{K_{oS}}{\rho_o}\left[f^2 + (K'_S - 4)f^3\right]. \tag{23}$$

The increase in energy along the isochore from the isentrope to the Hugoniot is obtained from the selected formulation of the Grüneisen parameter, since $\gamma \equiv V(\partial P/\partial E)_V$. For the conventional Mie-Grüneisen approximation, in which γ is constant along an isochore, this is a simple finite difference:

$$\Delta E_V = \frac{V}{\gamma(V)}(P - P_S). \tag{24}$$

In this work, when using the Mie-Grüneisen approximation we have assumed that $\gamma(V)$ is given by

$$\frac{\gamma(V)}{\gamma_o} = \left(\frac{V}{V_o}\right)^q, \tag{25}$$

In which the Grüneisen parameter at the reference state γ_o is known precisely from ultrasonic, thermal expansion, and heat capacity data and is a fixed parameter during fitting, whereas q is unknown and is a fitted parameter.

The solution of these equations for Hugoniot pressure at a given density, for the Mie-Grüneisen case, can be compactly written

$$P_H = \frac{P_S - \rho\gamma(\Delta E_S + \Delta E_{tr})}{1 - \frac{\gamma}{2}\left(\frac{\rho}{\rho_{oo}} - 1\right)}, \tag{26}$$

If the sample begins in the reference state, $\Delta E_{tr} = 0$. Hence equation (26) is used to compute both the hot liquid Hugoniot and the cold solid Hugoniot curves for the Mie-Grüneisen model.

Note that an alternative expression for γ is $\gamma = (\partial \ln T/\partial \ln V)_S$. Hence the temperature along an isentrope can be obtained by integrating this expression. For the Mie-Grüneisen case and the form of equation (23), we have

$$T_S = T_o \exp\left\{\frac{\gamma_o}{q}\left(1 - \left(\frac{\rho_o}{\rho}\right)^q\right)\right\}. \tag{27}$$

For the model introduced in this paper, $\gamma(E,V)$ is not a constant along the isochore from the isentrope to the Hugoniot and so we cannot use equation (24). In this model, we have adopted the form

$$\gamma(E,V) = \left(\frac{a}{V} + b\right)(E - E^*) + \gamma^*, \tag{28}$$

where a, b, E^*, and γ^* are the adjustable parameters. Note that the reference datum

$$\gamma(E_o, V_o) = \gamma_o \tag{29}$$

is added to the fit and assigned an extremely high weight, in order to enforce the known reference value of the Grüneisen parameter.

The relationship between pressure increase and internal energy increase along the isochore from the isentrope to the Hugoniot state is given in this case by

$$P - P_S = \frac{1}{V}\int_{\Delta E_S + \Delta E_{tr}}^{\Delta E_H} \gamma(E', V)\mathrm{d}E'. \tag{30}$$

In combination with equations (21) and (22), integrating the linear dependence on E from (28) yields a quadratic expression for P, of which one root is physical and one root is non-physical. With appropriate choice of ρ_{oo} and ΔE_{tr}, this quadratic solution yields either the Hugoniot from the hot liquid initial state or from the cold solid initial state, for the $\gamma(E,V)$ model.

Since the changes in both E and P with changes in V along the isentrope are known from equations (20) and (23), it is straightforward to obtain $\gamma(E,V)$ along the isentrope and hence to compute the temperature increase along the isentrope in this model as well.

The final equation that is relevant to fitting the model form to the experimental dataset for AnDi liquid incorporates the measurement of bulk sound velocity C_B in the shock state. As with any bulk sound wave, $C_B = \sqrt{VK_S}$, where again K_S is the isentropic bulk modulus. If the slope of the Hugoniot $(\partial P/\partial V)_H$ is obtained from the above equations by finite difference, then it can be shown that

$$K_S = \frac{1}{2}\left(\gamma P - \left(\frac{\partial P}{\partial V}\right)_H \left[2V - \gamma\left(\frac{1}{\rho_{oo}} - V\right)\right]\right). \tag{31}$$

The inversion for fitted parameters $\{K_S', a, b, E^*, \gamma^*\}$ is therefore based on γ_o, all twelve available preheated liquid Hugoniot shots, one cold solid aggregate Hugoniot shot, and one sound speed datum. All the constants $\{\rho_o, \rho_{os}, K_{oS}, \gamma_o, \Delta E_{tr}\}$ are given by Asimow and Ahrens (2010) but are repeated here for convenience: $\{2618\ \mathrm{kg\ m^{-3}}, 3078\ \mathrm{kg\ m^{-3}}, 22.98\ \mathrm{GPa}, 0.356, 1.954106\ \mathrm{MJ\ kg^{-1}}\}$.

0.6. Ergodicity check by mean squared displacement (MSD)

In liquid phase, particles follow the laws of Brownian mothion and their MSD is linear in time (namely, MSD $= 6Dt$ where D is the diffusion coefficient.) However, in glass phase,

the motion of the particles are confined by their neighbors and MSD increases more slowly with time. This phenomenon is called sub-diffusion and can be characterized by a slope lower than unity in a log-log plot of MSD *vs.* time.

To ensure the accuracy of the results, only ergodic MD simulations should be used in our thermodynamics calculations. We checked the MSD-t relationship for all simulations and excluded subdiffusive runs. Figure S1 shows two segments from our An-Di simulations highlighting the difference between liquid (diffusive) and glass (sub-diffusive) behavior. To avoid the superdiffusive region at the beginning of each simulation, both plots are based on the last 2.5 ns of 5-ns runs.

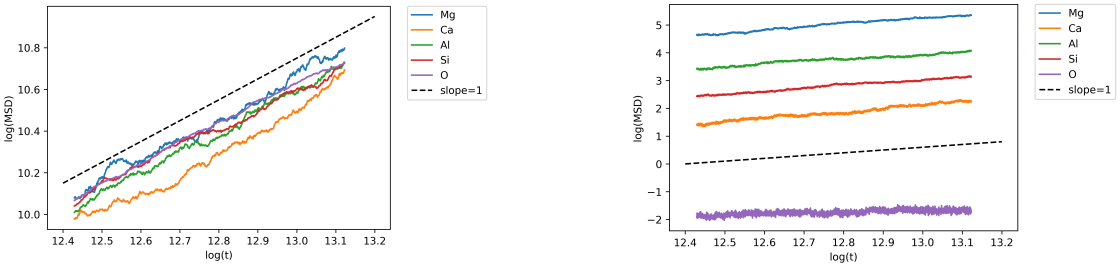

(a) Log(MSD)-log(t) for AnDi liquid

(b) Log(MSD)-log(t) for AnDi glass

Figure S1: Comparison of MSD plots of liquid-like and glass-like runs. (a) 6500 K, 1.5 GPa. Liquid-like behavior is indicated by slopes approximately equal to unity. (b) 2000 K, 150 GPa. Glass-like behavior is indicate by slopes much smaller than unity.

0.7. Thermal pressure coefficient

The thermal pressure coefficient $(\partial T/\partial P)_V = \alpha K_T$ is related to the Grüneisen parameter, which can be written $\gamma = V\alpha K_T/C_V$. When working with shock wave data, it is more convenient to use the Grüneisen parameter because data can be fit in energy space without reference to the heat capacity; when working with PVT data it is more convenient to use the thermal pressure coefficient. In any case, the Grüneisen parameter and the thermal pressure coefficient can each be functions only of volume, but only in the specific case that C_V is also a function of volume only. This is very unlikely to be the case; certainly it is not expected for models of heat capacity such as the Debye or Einstein models. Our simulations indeed show that C_V is a function of volume and energy. One might wonder whether all the energy dependence that we observe in gamma is then attributable to the energy dependence of C_V, but we find that C_V decreases with increasing energy at all volumes and so cannot explain the reversal in the slope of the energy dependence of gamma. Figure S2 shows the thermal pressure coefficient in our models. We find that the thermal pressure coefficient does not reduce to a simple function of volume only, especially at small volume (high pressure). The rate of decrease in thermal pressure coefficient with increasing temperature becomes more pronounced as volume decreases.

0.8. Fitting EOS to empirical simulation data

In the main text, equations of state based on a Birch-Murnaghan isentrope and either a Mie-Grüneisen or a $\gamma(E, V)$ thermal pressure model are fitted to experimental shock wave

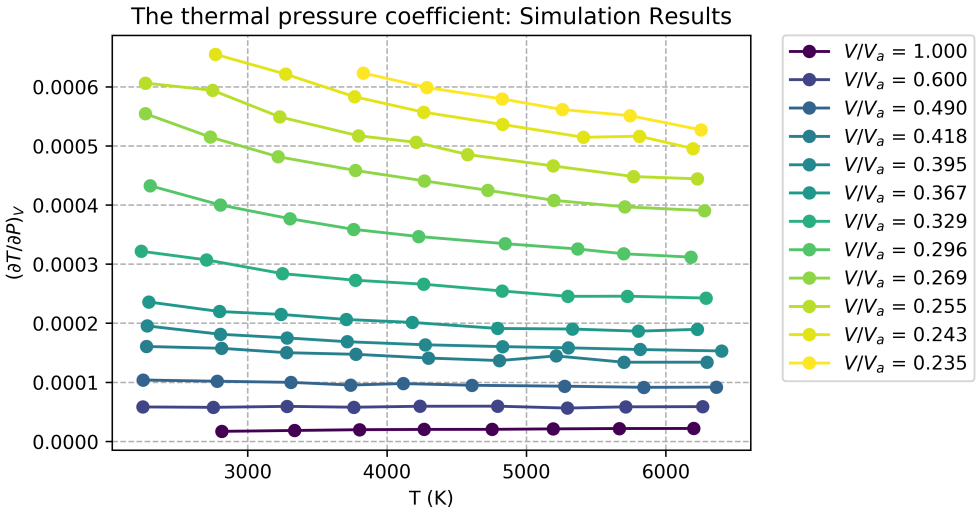

Figure S2: Thermal pressure coefficient isochores from the simulations of the present work.

data. Although the main purpose of our simulation campaign is to identify the general form of the EOS, here we also fit these functional forms to the EPMD simulation data themselves. We used the EPMD data at $V/V_a < 0.395$, i.e. $P > 10$ GPa, which are best tuned to the AIMD simulations. V_o was kept fixed in both models. For the Birch-Murnaghan plus Mie-Grüneisen model, we adjusted K_{S0}, K'_S, γ_0, and q to minimize the squared sum of residuals in pressure between the simulation points and the model at equal E and V. For the Birch-Murnaghan plus $\gamma(E,V)$ model, we similarly adjusted K_{S0}, K'_S, and the four parameters of the $\gamma(E,V)$ model. The results are shown in Figure S3 and Table S2. Although the differences are subtle, the $\gamma(E,V)$ model is a slightly better fit, with RMS error of 0.15 GPa vs. 0.17 GPa for the Mie-Grüneisen model.

Table S2: Comparison of the Birch-Murnaghan plus Mie-Grüneisen fit and the $\gamma(V, E)$ fit to EPMD simulation results.

Parameters	Mie-Grüneisen model	$\gamma(E,V)$ model
V_0 (m^3/kg)	0.0003820	0.0003820
K_{S0} (GPa)	21.95	24.68
K'_S	6.118	5.344
Model specific Parameters	$\gamma_0 = 0.521$ (at V_0) $q = -1.5$	$\gamma^* = 0.412$ $E^* = -2.04 \times 10^7$ J/kg $a = -1.95 \times 10^{-11}$ m^3/J $b = 4.43 \times 10^{-8}$ kg/J ($\gamma_0 = 0.548$ at V_0, E_0)

V_0 is the reference volume at 1 bar, 1673 K.

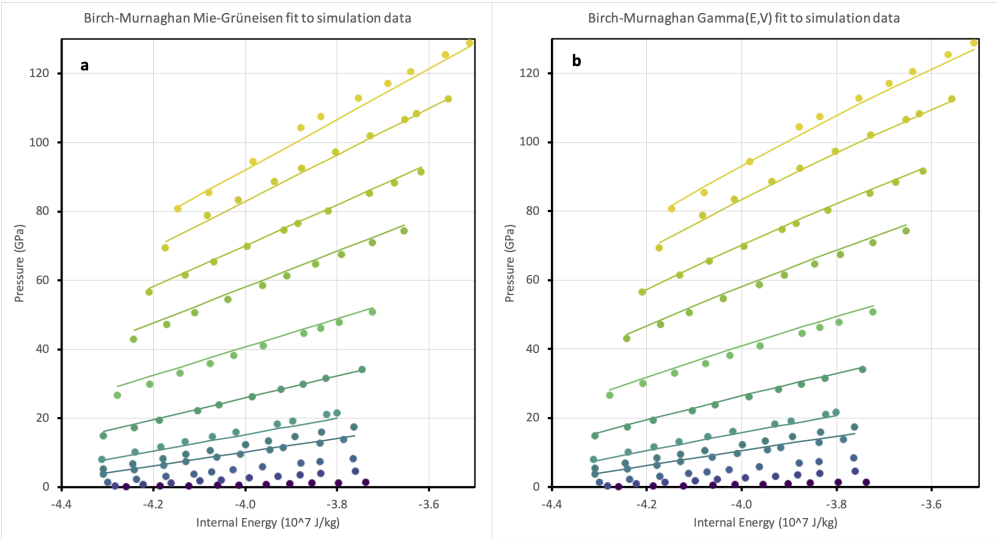

Figure S3: Fits of two EOS forms to the high-pressure subset of EPMD data, in pressure vs. internal energy space. (a) A Birch-Murnaghan isentrope plus a Mie-Grüneisen thermal pressure. (b) A Birch-Murnaghan isentrope plus a $\gamma(E, V)$ thermal pressure model. Colors of simulation points and EOS fit lines correspond to volumes as in Figures 1 and 3 in the main text.

0.9. Sample LAMMPS input files

Below is a sample input file showing how we used the new force field to calculate one NVT sample point.

```
# lammps input file for NCMAS melts simulation

# VARIABLES
variable        i               index   3000
variable        restart_name    index   nvt.3500.restart
variable        settings_name   index   scaled_matsui.in.settings
variable        log_name        index   3000.log
variable        nSteps_ramp     equal   1000000 # time for each annealing
   period. slow=1ns
variable        avg_freq        index   200
variable        coords_freq     index   200
variable        dump4avg        index   10
variable        T1              equal   3500 # Temperature during the
   initial anneal
variable        T2              equal   3000 # Temperature during the
   final anneal

# Change the name of the log output #
log ${log_name}

#=========================================================
# GENERAL PROCEDURES
#=========================================================
units   real  # g/mol, angstroms, fs, kcal/mol, K, atm, charge*angstrom
```

```
dimension 3 # 3 dimensional simulation
newton    off # use Newton's 3rd law
boundary  p p p # periodic boundary conditions
atom_style  charge    # charge (for ions: coordinates, velocities, atom IDs, types, charges)

#============================================================
# FORCE FIELD DEFINITION
#============================================================
pair_style     buck/coul/long 11.0  # outer_Coul (cutoff values, see LAMMPS Doc)
kspace_style   pppm 0.0001          # long-range electrostatics sum method

#============================================================
# SETUP SIMULATIONS
#============================================================

# READ IN COEFFICIENTS/COORDINATES/TOPOLOGY
read_restart ${restart_name}
include ${settings_name}

# SET RUN PARAMETERS
timestep  1.0   # fs
run_style verlet    # Velocity-Verlet integrator
neigh_modify every 1 delay 0 check no # More relaxed rebuild criteria can be used

#============================================================
# THERMO
#============================================================
# DECLARE RELEVANT OUTPUT VARIABLES
variable   my_step   equal   step
variable   my_temp   equal   temp
variable   my_vol    equal   vol
variable   my_rho    equal   density
variable   my_etot   equal   etotal
variable   my_pe     equal   pe
variable   my_coul   equal   ecoul
variable   my_long   equal   elong
variable   my_evdw   equal   evdwl
variable   my_ent    equal   enthalpy
variable   my_P      equal   press

fix  averages all ave/time ${dump4avg} $(v_avg_freq/v_dump4avg) ${avg_freq} v_my_temp v_my_vol v_my_rho v_my_etot v_my_pe v_my_coul v_my_long v_my_evdw v_my_ent v_my_P file thermo.$i.avg

#============================================================
# EQUILIBRATE THE BOX BY NPT RUN
#============================================================
```

```
dump equil all custom ${coords_freq} equil.$i.lammpstrj id type xu yu zu
   vx vy vz
dump_modify equil sort  id
fix equil all nvt temp ${T1} ${T2} 100.0

run   ${nSteps_ramp}

unfix equil
undump equil
unfix averages

# WRITE RESTART FILES
write_restart   nvt.$i.restart
write_data      nvt.$i.data
```

Below is the the input file describing our new force field. (*scaled_matsui.in.settings* mentioned in line 6 in the previous file)

```
 # Non-bonded interactions (pair-wise)
pair_coeff   1   1   314506743771.52  0.08  400.0067
pair_coeff   1   2   11313599738.4  0.08  284.0429
pair_coeff   1   3   365404704482.73  0.08  439.9976
pair_coeff   1   4   19288912785.37 0.074 360.0158
pair_coeff   1   5   578091787566.03  0.063 482.0418
pair_coeff   1   6   52943434.3862237 0.109451274814982 78.9992138379116
pair_coeff   2   2   406978678.76 0.08  201.6975
pair_coeff   2   3   13144527584.6  0.08  312.4402
pair_coeff   2   4   529901504.2  0.074 255.6456
pair_coeff   2   5   8478304051.37  0.063 342.2957
pair_coeff   2   6   5030841.14729292 0.111200388183525 54.4266683653554
pair_coeff   3   3   424539698122.04  0.08  483.9866
pair_coeff   3   4   22684743951.5  0.074 396.0086
pair_coeff   3   5   699390225204.21  0.063 530.2342
pair_coeff   3   6   55601206.5371633 0.109479300137684 86.8482972553961
pair_coeff   4   4   728042565.29 0.068 324.023
pair_coeff   4   5   16878915502.56 0.057 433.8494
pair_coeff   4   6   2499266.0433064  0.10926898033415  67.374133749643
pair_coeff   5   5   1843386062908.58 0.046 580.9011
pair_coeff   5   6   3821560.4434135  0.102832132904819 89.6631707406477
pair_coeff   6   6   351953.268667045 0.24517533166497  1159.41353486781
```

References

Asimow P.D. and Ahrens T.J. (2010) Shock compression of liquid silicates to 125 GPa: The anorthite-diopside join. *J. Geophys. Res. B: Solid Earth* **115**.

Gilbert T. (1968) Soft-sphere model for closed-shell atoms and ions. *J. Chem. Phys.* **49**, 2640–2642.

Matsui M. (1998) Computational modeling of crystals and liquids in the system Na_2O-CaO-MgO-Al_2O_3-SiO_2.*Geophys. Monogr. Ser.* **101**, 145–151.

Mayo S.L., Olafson B.D. and Goddard W.A. (1990) Dreiding: a generic force field for molecular simulations. *J. Phys. Chem.* **94**, 8897–8909.

Wolfram Research, Inc. (2020) Mathematica, Version 12.2 Champaign, IL.